Journal of Power Sources 213 (2012) 255–264

Contents lists available at SciVerse ScienceDirect

Journal of Power Sources

journal homepage: www.elsevier.com/locate/jpowsour

An aqueous electrolyte, sodium ion functional, large format energy storage device for stationary applications

J.F. Whitacre [a,b,*], T. Wiley [a], S. Shanbhag [a], Y. Wenzhuo [a], A. Mohamed [a], S.E. Chun [b], E. Weber [a], D. Blackwood [a], E. Lynch-Bell [a], J. Gulakowski [a], C. Smith [a], D. Humphreys [a]

[a] Aquion Energy, 32 39th Street, Pittsburgh, PA 15201, USA
[b] Department of Materials Science and Engineering, Department of Engineering and Public Policy, Carnegie Mellon University, Pittsburgh, PA 15213, USA

ARTICLE INFO

Article history:
Received 3 January 2012
Received in revised form
16 March 2012
Accepted 7 April 2012
Available online 16 April 2012

Keywords:
Sodium-ion battery
Aqueous electrolyte hybrid device
Asymmetric energy storage device
Stationary energy storage
Lead acid battery
Renewable energy storage

ABSTRACT

An approach to making large format economical energy storage devices based on a sodium-interactive set of electrodes in a neutral pH aqueous electrolyte is described. The economics of materials and manufacturing are examined, followed by a description of an asymmetric/hybrid device that has λ-MnO_2 positive electrode material and low cost activated carbon as the negative electrode material. Data presented include materials characterization of the active materials, cyclic voltammetry, galvanostatic charge/discharge cycling, and application-specific performance of an 80 V, 2.4 kW h pack. The results indicate that this set of electrochemical couples is stable, low cost, requires minimal battery management control electronics, and therefore has potential for use in stationary applications where device energy density is not a concern.

1. Introduction

As the electricity grids of the world age and grow, and as renewable power sources (such as solar arrays, wind turbines, micro sterling engines, solid oxide fuel cells) proliferate, there is an increasing need for large-scale secondary (rechargeable) energy storage capability. Both distributed and centralized systems are needed, with storage capabilities ranging from under 10 kW h to 100's of MW h's. Batteries for these stationary applications are typically based on the lead acid, sodium sulfur (NaS), or Li-ion chemistries, and to date there are 100's MW of installed storage capacity for a total of 1000's of MW h globally. Further, it is predicted that the global annual market for stationary storage will exceed 30 $B by 2021 [1].

While current state-of-the-art batteries are functional and appealing for some applications, there is still a need for a lower cost, more stable, completely environmentally benign, longer-lived chemistry. Proposed solutions include a range of flow batteries [1,2], low cost Li-ion chemistries [3], advanced lead acid [4], and next generation sodium sulfur [5]. Of these, it is not apparent which will be able to be manufactured in a timely fashion at the right cost at the required scale.

The approach described here represents what we believe is the first demonstration of scaled production of large format (>30 W h), aqueous electrolyte, asymmetric energy storage cells that are then connected to make large-scale systems. To minimize cost, only the cheapest raw materials were considered during the development phase. This selection criterion narrowed the possible materials that might be used in the device significantly, and of those options identified, few held promise. After a substantial screening effort, several promising anode and cathode compounds were identified, and further exploration of these led to the device described here. It was also concluded that a neutral pH aqueous electrolyte would be most appealing from a manufacturing and cost perspective provided that sufficient energy density could be created in the device. Recent results published in the asymmetric/hybrid energy storage device literature have shown that high cell potentials, sometimes exceeding 2 V, and excellent cycle stability, in the 10,000's of cycles, can be achieved using this type of device [6–10]. These results show that the number of cycles required for cost effective use are in fact possible, and it also indicates that the common degradation mechanisms observed in Li-ion and lead acid batteries are not present. Table 1 summarizes these results, which

* Corresponding author. Department of Materials Science and Engineering, Department of Engineering and Public Policy, Carnegie Mellon University, Pittsburgh, PA 15213, USA. Tel./fax: +1 412 2684458.
E-mail address: whitacre@andrew.cmu.edu (J.F. Whitacre).

0378-7753/$ – see front matter © 2012 Elsevier B.V. All rights reserved.
doi:10.1016/j.jpowsour.2012.04.018

Table 1
Listing of other aqueous electrolyte devices with interaction-type cathodes that have demonstrated significant cycle life stability.

Cathode material	Functional cation	Specific capacity	# Cycles with little to no loss	Ref
Copper hexacyanoferrate	K	40–50 mA h g^{-1}	40,000	[8]
Sodium birnessite	Na	25–30 mA h g^{-1}	>2000	[6,10]
$Na_4Mn_9O_{18}$	Na	45 mA h g^{-1}	>2000	[15]
Lithium manganate (cubic spinel)	Li	100 mA h g^{-1}	20,000	[7]

serve to further support the idea that a long-term/stable chemistry with an extremely slow materials degradation mechanism is possible.

In our case, the cathode (positive electrode) consists of λ-MnO_2, which is the cubic spinel phase commonly produced via the lithiated compound $LiMn_2O_4$ [11]. The electrolyte contains 1 M Na_2SO_4. The anode is a low cost activated carbon and the rest of the battery device can be composed of simple packaging and current collection materials. Because an aqueous electrolyte is used, thick format (>1 mm) electrodes are feasible since ion conduction in aqueous media is sufficiently fast to enable long-range ionic motion during reasonable charge/discharge rates. Data from devices ranging from simple coin cell test fixtures through large format units suggest that the approach is viable and that a low cost stationary energy solution based on this type of device is feasible. This paper contains a description of this technology and discloses the performance of industrially scaled devices under different use conditions. Fundamental electrochemical and materials results that support the findings here can be found in referenced and forthcoming articles.

2. Experimental details

2.1. Materials selection criteria

For stationary storage applications, the two most important device parameters are capital cost (at an installed cost per usable W h basis) and system longevity (through which the capital cost is amortized via cycling through the usable energy storage). Also important are efficiency and environmental impact. Energy density and specific energy are less important provided that the minimal necessary requirements are met; the majority of the stationary applications do not have particularly limiting volume or mass constraints (particularly if co-located with solar or wind assets).

It is often posited that for stationary storage to be economically viable, the capital cost of the storage itself should be less than \$200 kW h^{-1} and should approach \$100 kW h^{-1} to be truly disruptive. Fig. 1 illustrates the relationship between the energy-normalized cost (\$ kW h^{-1}), specific energy of the device (W h kg^{-1}), and the mass-normalized average cost of the goods sold (COGS) of the battery device (\$ kg^{-1}), in Fibonacci increments. The simple assessment in Fig. 1(a) shows that as the COGS value increases, it is very difficult to approach \$100 kW h^{-1}. In fact, if the average device materials cost exceeds \$50 kg^{-1}, the specific energy must exceed 400 W h kg^{-1} at a device level (including active and inactive materials) to approach a specific cost of \$100 kW h^{-1}. As a case in point, Fig. 1(b) shows the relationship between energy density and mass-normalized COGS if a \$100 kW h^{-1} constraint is applied. The challenge at hand when considering existing technologies is then evident: only a handful of battery chemistries have specific energy values in excess of 100 W h kg^{-1} at the device level. Any storage technology that has a specific energy <100 W h kg^{-1}, then, must have a total mass-normalized COGS of less than

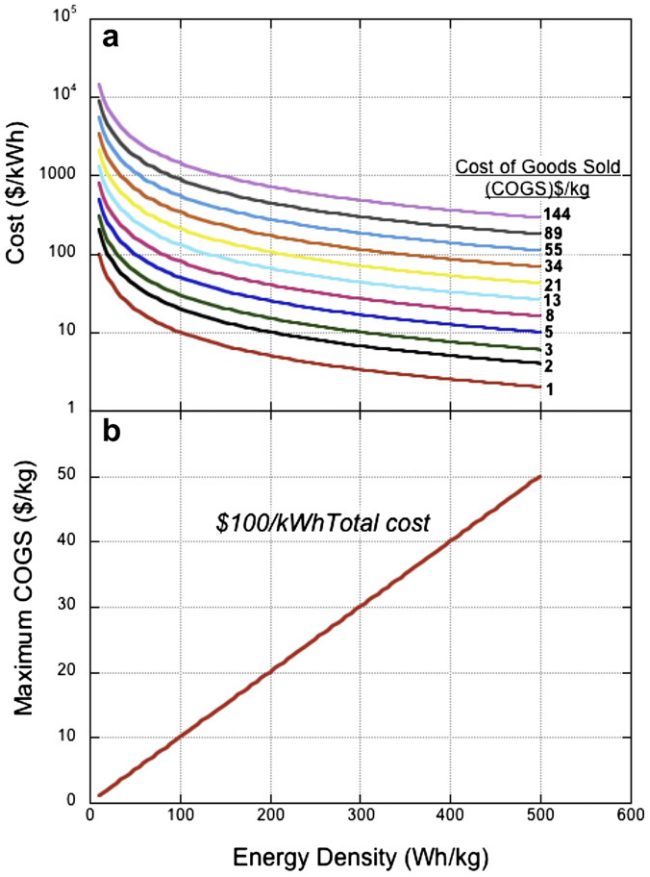

Fig. 1. Plots that indicate the relationship between energy device cost in \$ kW h^{-1}, cost of goods sold (GOGS), and energy density.

\$10 kg^{-1} to meet the \$100 kW h^{-1} target. This specific cost value is substantially lower than the well-documented mass-averaged cost for nearly every battery system, with the lead acid chemistry being perhaps the only exception.

A second key consideration when determining the economic viability of an energy storage device is system longevity, as assessed both in terms of both available duty cycles and calendar time. A bulk energy storage unit will only be implemented if it is cost effective over a reasonable time frame. That is to say that the levelized cost of stored electricity (LCSE) in \$ kW h^{-1} discharged must make financial sense for a range of applications. The value of stored electricity is highly variable and depends on many factors, however for multi-hour bulk energy storage it is suggested here that the LCSE should be below \$0.03 kW h^{-1}, a value lower than the cost of electricity from conventional power sources (such that the premium for storing the electricity is not prohibitively expensive). This implies that the device must be able to deliver many thousands of charge discharge cycles over many years. The number of cycles varies dramatically depending on use case, however we suggest here that a storage solution needs to exhibit at least 5000 and more likely 10,000 full cycles over 5–15 years.

This becomes relevant for functional materials selection when considering the fact that the energy density of a material is thermodynamically linked to the change in free energy and configurational entropy experienced during electrochemical cycling. The more energy per mass that can be inserted and extracted from a secondary battery active material during cycling, the more change it must undergo. In general, the more change an energy storage material undergoes during a use cycle, the more apt it will be to lose

function over that cycle. More simply: cycle life for secondary battery electrode materials will commonly have an inverse correlation with energy density, and so to achieve very high cycle life (over 10,000 cycles), lower energy density materials systems (under ~50 W h kg^{-1}) should be considered as a rule. Combining this notion with the information represented in Fig. 1, we were driven to develop relevant materials for stationary storage that cost less than \$5 kg^{-1} while delivering between 20 and 50 W h kg^{-1} over multiple 1000's of cycles.[1]

2.2. Materials screening and selection methodology

2.2.1. Electrolyte selection

The above constraints and findings suggest that an aqueous electrolyte should be suitable for use. Water is a much less costly solvent compared to the organic solvents used in Li-ion chemistries, and ionic transfer through aqueous solution can be more than an order of magnitude better than that observed in other types of electrolytes. Further, the idea of using neutral pH or near-neutral pH solutions has significant appeal from a manufacturing and lifetime perspective, since minimizing possible sources of corrosion is a concern. For this reason, aqueous solutions of sodium − sulfates, nitrates, and ammoniates were selected as a starting point for investigation.

2.2.2. Cathode material

It is clear that only a small number of well-studied electrochemical cathode materials can be manufactured in bulk within the adopted cost constraints. Of these, manganese oxide materials are particularly appealing given the extremely abundant nature of electrolytic manganese dioxide (EMD) and its low cost (less than \$2 kg^{-1} if purchased in bulk). Because intercalation reactions are more reversible and more stable than classical electrode surface phase change reactions (and electrode stability is of substantial concern), Mn-based intercalation compounds are of particular interest. Furthermore, given the electrolyte selection and cost constraints, finding a MnO_x compound capable of intercalating sodium at either anodic or cathode potentials would seem to offer a particularly attractive solution.

There are many stable phases of MnO_2, including α, γ, and birnessite [12,13]. One phase, the orthorhombic $Na_4Mn_9O_{18}$, has been described as possible Na-ion material for organic electrolyte cells, and also as a templated material for Li-ion use. We found that it had excellent electrochemical stability in a 1 M aqueous sodium sulfate solution, while delivering over 1000 full cycles with no fade in delivered capacity [14,15]. This material was able to deliver between 30 and 40 mA h g^{-1}, a satisfactory but somewhat low value.

Further investigation showed that a different phase, the cubic spinel λ-MnO_2 system was able to function well in a sodium sulfate solution and could deliver a specific capacity of up to 100 mA h g^{-1}. While this material contains Li as produced, a cost/performance assessment using verified materials prices and processing routes shows that the specific cost, in \$ A h^{-1}, is significantly less for lithium-templated λ-MnO_2 than for the $Na_4Mn_9O_{18}$ material, and that this relationship will hold even if the cost of bulk Li_2CO_3 is as high as \$10 kg^{-1} (it is currently well under \$5 kg^{-1} from some sources as purchased in large lots). A further finding concerning the λ-MnO_2 system is that it is completely stable in the aqueous electrolyte; the most commonly sited degradation mechanisms for this material, the evolution of corrosive HF in organic solvent electrolytes with F containing salts, does not occur. For this reason, the λ-MnO_2 does not require the doping, unusual processing, or surface coatings found appealing for $LiMn_2O_4$ in organic solvent cells. This result is well supported by other work that uses $LiMn_2O_4$ in aqueous electrolytes with Li-based salts, where tens of thousands of full cycles have been demonstrated with little to no capacity fade and greatly decreases the processing/synthesis cost of this material [14,15].

2.2.3. Anode materials

The half-cell potentials encountered under anodic conditions for a neutral pH aqueous system are corrosive to most potential materials systems. However, in order to achieve the highest possible cell voltage, it is desirable to have electrodes that function at or beyond the potential of water electrolysis. Many metal-oxide ceramic materials possess the desired intercalation functionality within appropriate potential windows. However, these materials have not been found to be stable over the number of cycles demanded by the stationary application, with the best results being in the 100's of cycles prior to failure in aqueous electrolyte Li-ion devices [16]. This is likely because of the corrosive environment provided by locally evolved OH− under anodic conditions.

Carbon, however, is exceedingly stable in aqueous media, and is also very resistant to corrosion under extreme conditions. Carbon also has unusually high overpotential for water electrolysis and is known to have a stable interface and have a charge storage function in aqueous electrolytes at potentials well below −1 vs. Hg/Hg_2SO_4. There are a variety of theories that might explain how this is possible, the most plausible being that evolved hydrogen is stored locally inside of or on the carbon electrode and recombines with local OH− groups upon discharge [17–20]. This hydrogen storage effect would not be classified as pseudocapacitance, since it involves the evolution and consumption of a secondary functional species, however the resulting performance metrics are consistent with those observed in materials that do exhibit pseudocapacitance. High surface area activated carbons and/or surface modified carbons that demonstrate pseudocapacitive and possible hydrogen storage behaviors are therefore very appealing provided they could be produced at a sufficiently low price.

Typical carbons made for electrochemical double layer capacitors, or "super capacitors", can have specific capacitance values over 200 F g^{-1}, but are made using costly precursors and processing routes and are tailored for use in organic solvent based devices (where water is an impurity, and the aforementioned hydrogen evolution/storage mechanism does not occur). There are, however, other classes of lower cost carbons that have sufficient capacitance. For example, it has been demonstrated that devices with specific capacitance values exceeding 200 F g^{-1} in an aqueous Na_2SO_4 can be made starting with low cost food-grade carbohydrates using several processing routes [21]. Other results indicate that adding small amounts of pseudocapacitive material to an activated carbon carrier can significantly increase capacity and performance [22].

2.3. Description of materials, cells, and batteries

2.3.1. Active materials synthesis

Positive electrode material: Cubic spinel λ-MnO_2 was synthesized by first creating $LiMn_2O_4$ followed by electrochemical or chemical delithiation. Li_2CO_3 was ball milled with electrolytic manganese dioxide (EMD, Tronox) (Spex 8000, silicon nitride crucible) or attritor milled (Union Process, 2 mm diameter media) in the proper molar ratio for 60–120 min. This precursor mix was fired at

[1] A notable exception of this rule is for elemental electrode materials that have simple alloy/dealloying reactions and are kept in a liquid phase during use such as the sodium sulfur or sodium nickel metal halide chemistries. While these chemistries are stable over many cycles, they must be kept hot (above approximately 300 °C) continuously and so have a variety of drawbacks in many use cases.

750–800 °C in ambient air for 8–12 h with heating and cooling ramp rates of 5 °C min^{-1}. Phase purity was verified with X-ray diffraction data from the solid-state synthesized material with the predicted JCPDS included for comparison, while the SEM analysis showed the expected clusters of sub-micron particles, as is common for this material. In some cases, trace amounts of unreacted Mn_2O_3 (which originates from EMD that converts to Mn_2O_3 at elevated temperatures) that is electrochemically inert was observed.

Negative electrode material: Activated carbon was created as described elsewhere [21]. α-D-glucose (also known as dextrose, or corn syrup) (ACROS ORGANICS) precursor was dewatered in air atmosphere at 185 °C for 24 h. The resulting caramelized glucose was then ground into powder particles until all of the particles passed through a 300 μm mesh screen. The caramelized glucose powder was pyrolyzed under flowing Ar gas in a horizontal tube furnace with a heating rate of 5 °C min^{-1} and held at a pyrolysis temperature of 600 °C for 2 h. This pyrolyzed glucose was again ground into the powder and passed through a 300 μm mesh. The carbon was then infiltrated with KOH via soaking in a solution where etching agent is mixed with the KOH/carbon mass ratio of 4:1 for 1 h. The impregnated slurry was dried at 110 °C for 12 h and then activated at 800 °C in a horizontal tube furnace under flowing Ar for 2 h with a heating/cooling rate of 5 °C min^{-1}. The resultant activated carbon specimens were rinsed with 0.5 M HCl to remove residual activating agent and washed out with hot de-ionized water repeatedly until the pH of outlet water reached 6.

Electrode Production: Thick format freestanding electrodes were made by first mixing active materials with a binder (PTFE) and some conductive additives (graphite and/or carbon black). The anode mixture typically has more than 90 mass% active material (activated carbon), while the cathode typically has more than 85 mass% active material. The mixture was then either rolled or die pressed into electrode units that can be combined to make individual cells or can instead be assembled into batteries that have either a bipolar or prismatic parallel architecture [15].

The separator materials consist of nonwoven cotton or synthetic fiber filtration paper. Coin cells with varying dimensions were constructed, including 2032, 2450, and 2477. In these cases, current collection was achieved simply by the coin cell casing. Very thick electrode cells were created using a simple PTFE swagelock-based cell.

Larger format cells were created using machined or injection molded acrylic or polypropylene fixtures with a combination of graphite sheeting and 316 or 304 stainless steel foil as current collection/tabbing. Package sealing was accomplished either through pressurized o-ring structures or through melt sealing (laser welding or hot plate). In some cases the electrodes were soaked in the electrolyte (1 M Na_2SO_4) prior to assembly, while in other cases, the cells or batteries were assembled first and then infiltrated with electrolyte using an industrial process similar to that used in the lead acid industry.

Very large stacked prismatic devices with a capacity in excess of 30 A h (20 h rate) were assembled in custom-designed injection molded polypropylene cases. Current collection was done via graphite sheeting, while spot-welded stainless steel tabs were used to interconnect the true prismatic layers to stainless steel terminal structures.

3. Results

3.1. Performance of λ-MnO_2 cathode material in aqueous Na_2SO_4

The cubic spinel λ-MnO_2 material had excellent energy storage functionality in aqueous Na_2SO_4 solution. Fig. 2 depicts the improvement of this material over the previously described orthorhombic $Na_4Mn_9O_{18}$ material [14,15]. The data in this figure were collected in two similar cells that had the same activated carbon anode material and an optimized anode/cathode mass ratio to support a 1.8 V full charge voltage [7]. The cubic spinel material was able to offer a greater than 2 fold increase in specific capacity and a nearly 3× increase in specific energy. Both materials were made by a nearly identical solid-state synthetic route, and the only significant difference between these two materials was the use of Li_2CO_3 instead of Na_2CO_3 during precursor mixing.

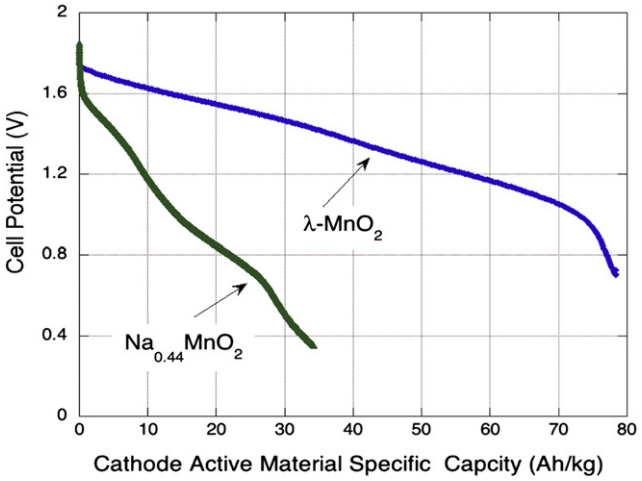

Fig. 2. Discharge curves from two different manganese-based cathode materials as cycled in an aqueous solution of 1 M Na_2SO_4: $Na_4Mn_9O_{18}$ and λ-MnO_2. The λ-MnO_2 had much more capacity and energy density.

3.2. Activated carbon positive electrode material

Fig. 3 shows a collection of data from carbons produced starting from the carbohydrate precursor glucose D (or dextrose; corn syrup). Using this class of materials as a precursor has the benefit of having very low impurity content while also costing very little. Results show that, if the material is processed under the proper

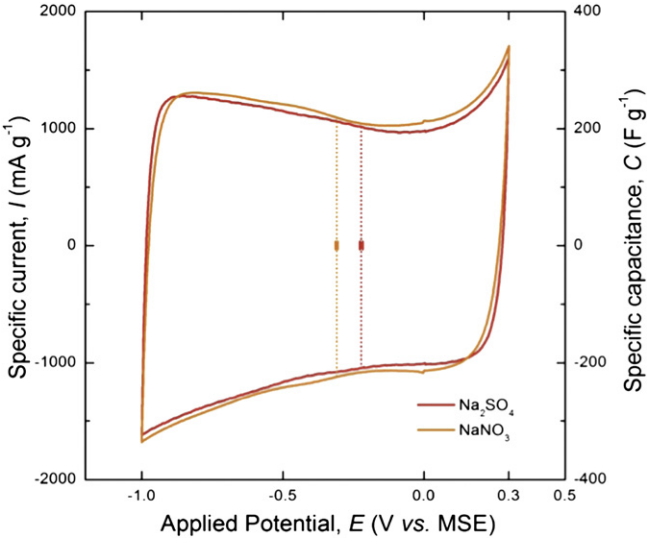

Fig. 3. Cyclic voltammetry showing the capacitive performance of activated carbon derived from low cost carbohydrate precursor. In this case, the scan rate was 5 mV s^{-1}, and the sample was tested in aqueous solutions of 1 M Na_2SO_4 and $NaNO_3$. A specific capacitance of over 200 F g^{-1} was observed.

conditions, specific capacitance values greater than 225 F g^{-1} can be achieved in neutral pH electrolytes with either Na_2SO_4 or Na_2NO_3 as a salt [21]. While processing these carbons is still relatively costly if a KOH activated step is required, alternative routes are possible that include hydrothermal synthesis, NaOH activation, and carbon surface modifications with pseudocapacitive species. These results are under preparation for publication in a separate manuscript.

3.3. Thin format cell performance

Coin cell format devices with electrodes less than 100 μm in thickness were produced with anode/cathode active materials mass ratios of approximately 1.2–1. Electrodes with this dimensionality will exhibit very little potential loss to electronic and ionic polarization, thus allowing for the absolute potential of the active material to be assessed. Fig. 4 shows characteristic charge/discharge voltage profiles under potential-limited galvanostatic charge and discharge cycling between 1.6 and 0.6 V. The potential response under three different current loadings is plotted in Fig. 4(a), while Fig. 4(b) shows the round trip columbic and total energy efficiency (% of charge energy retained during discharge). The current loading in terms of C-rate[2] is indicated at the bottom of the plot. The round trip energy efficiency was excellent in this case: greater than 95% for a 2C cycling rate and in excess of 90% for current loadings as high as 6C.

3.4. Thick format cell performance

To minimize device cost, it is imperative that the electrodes employed be as thick as possible. This allows for the greatest amount of active material to be used per unit mass of ancillary materials (packaging, current collection, etc.). However, there are inherent limits to practical electrode thicknesses due to the physics of electronic and ionic transport through electrolyte and porous bodies. The ionic conductivity of alkali ions in water-based electrolytes is typically at least an order of magnitude better than that observed in solvent based electrolytes as used in Li-ion systems. In principle, this allows for electrodes that are much thicker than those typically used in Li-ion batteries. Fig. 5 shows that it is possible to extract substantial energy density values from thick format electrodes (multi-millimeter). In this case, a glucose-derived activated carbon anode (6 mm thick) was paired with a λ-MnO_2 cathode (3 mm thick) in an approximate 1:1 mass ratio. The electrodes were 15 mm diameter pellets that were tested in a Teflon swage-style cell with stainless steel current collectors. In a 1 M Na_2SO_4 electrolyte, the device was able to deliver an energy density of 25 W h l^{-1} under 5 h. While this value is lower than many existing battery chemistries, it is also significantly higher than many stationary storage solutions under consideration such as some flow batteries, fly wheels, and compressed gas based approaches [23]. This same device attained a total specific energy of 23 W h kg^{-1} for the test shown.

3.5. Graphite sheet – based current collection

Another key device level cost driver for aqueous electrolyte batteries can be found in current collector materials. In many cases, high-cost corrosion-resistant materials must be used to transport electronic current into and out of the electrode stack. To this end, we have investigated the promise of using low cost graphite sheeting instead. While the resistivity of graphite is significantly higher than that for metallic materials, the current densities within are low enough in this device such that the I^2R losses are acceptable when the devices is charged/discharged at areal current densities corresponding to those needed to drive multi-hour charge/discharge conditions. Fig. 6 shows data from a test cell that was made using only graphite sheet for current collection with large area 5 cm diameter electrodes (total cell thickness, anode + cathode, was 7 mm). In this case, graphite foil 100 μm in thickness was used for both anode and cathode current collection without any locally applied metal. Fig. 6(a) shows the charge/discharge voltage vs. capacity profiles for the device for current levels ranging from C/2 to

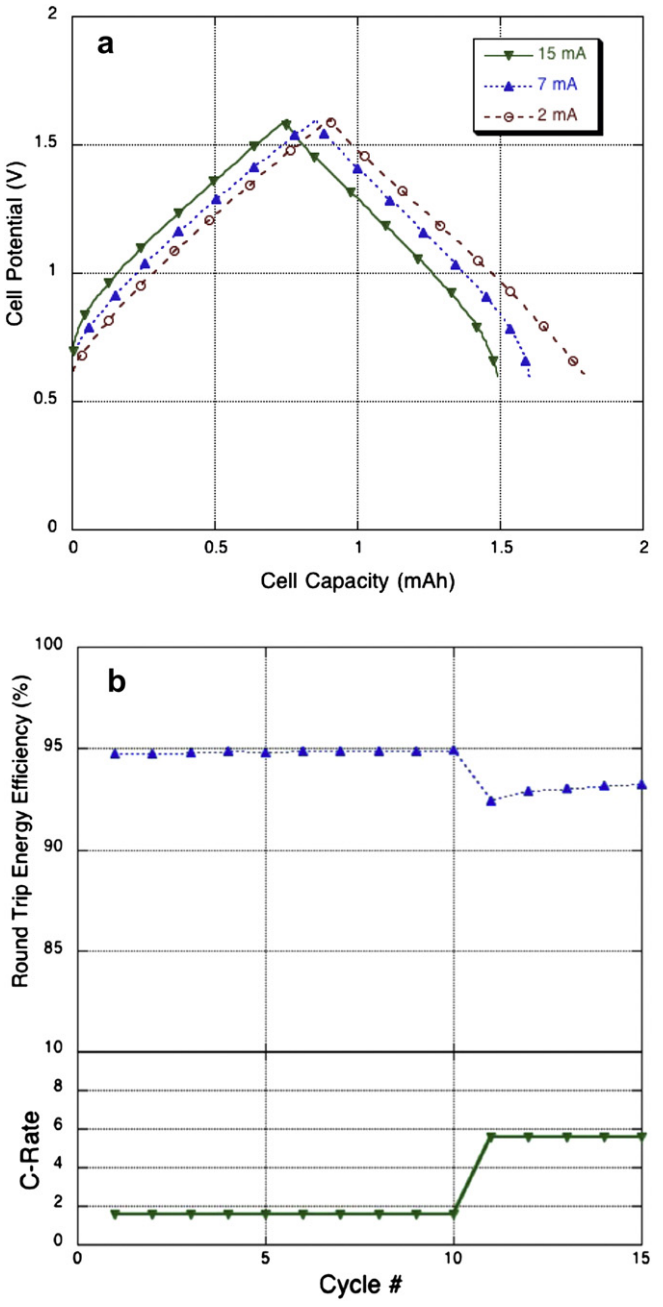

Fig. 4. (a) Galvanostatic, potential-limited charge discharge curves for full cells made with λ-MnO_2 positive electrode and an activated carbon negative electrode. (b) Round trip energy efficiency as a function of cycle and C-rate for thin electrode cells. Efficiencies of up to 95% were documented for a cycling rate of 2C.

[2] The C-rate number is the value by which the capacity value, (in Ah), is multiplied by to arrive at the magnitude of the applied current (in A) – so a 2C rate on 1 Ah battery is 2 A and so on.

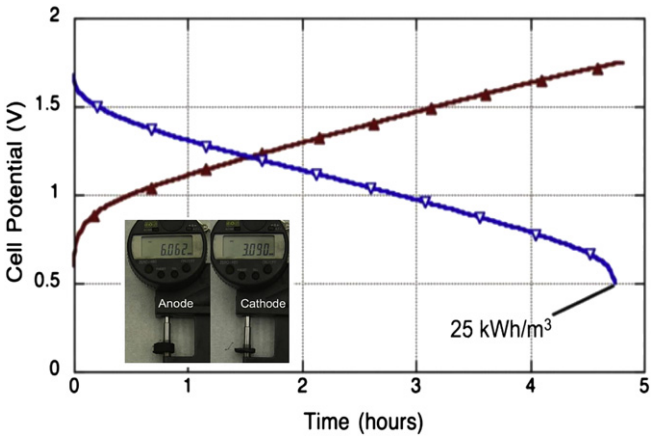

Fig. 5. Charge/discharge curve recorded from a thick electrode cell made. Total cell thickness approached 1 cm, and an electrode-level energy density of 25 W h l^{-1} (kW h m^{-3}) could be reversibly extracted in less than 5 h of discharge.

C/15. Fig. 6(b) documents the relationship between fractional delivered energy as a function of discharge time. The data indicate that for energy storage cycles longer than 2 h in charge or discharge duration, over 80% of the ultimate cell capacity can be extracted. Furthermore, the magnitude of the electronic polarization is small (less than 50 mV) in the range of areal current densities used, which was approximately 1–10 mA cm^{-2}.

3.6. Cycle life and longevity

The long-term stability of the device is measured using both high rate/short duration cycling, as well as lower rate cycling to 100% depth of discharge. Fig. 7(a) shows the low rate charge discharge performance under galvanostatic cycling conditions of a 12 A h unit. The voltage vs. time profile is stable, with each cycle essentially identical to the previous even under very deep discharge, low rate testing conditions. Fig. 7(b) shows the performance of a fully sealed 200 mA h cell cycled under similar conditions for 12 months at a ~6 h charge/discharge rate (approximately 2 galvanostatic charge/discharge cycles per day). Beyond seasonal thermal variation, no loss in capacity was observed throughout the test. Furthermore, the columbic efficiency of the cell was >99% for each cycle. To test the electrochemical junction's tolerance to

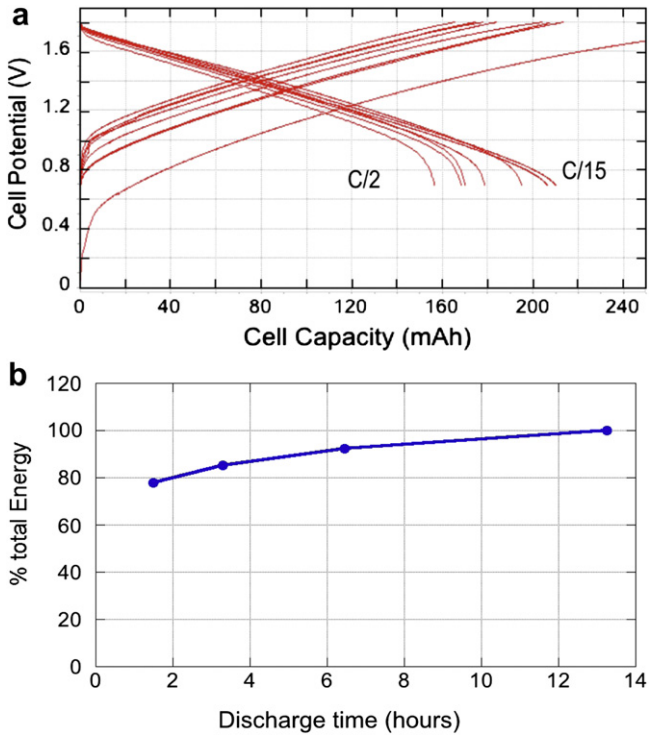

Fig. 6. (a) Potential-limited Galavanostatic charge/discharge data from a "metal free" device that used only graphite sheet for current collection. The charge/discharge current rates ranged from C/2 to C/15. (b) Plot indicating % of the C/15 rate embodied energy as a function of discharge time.

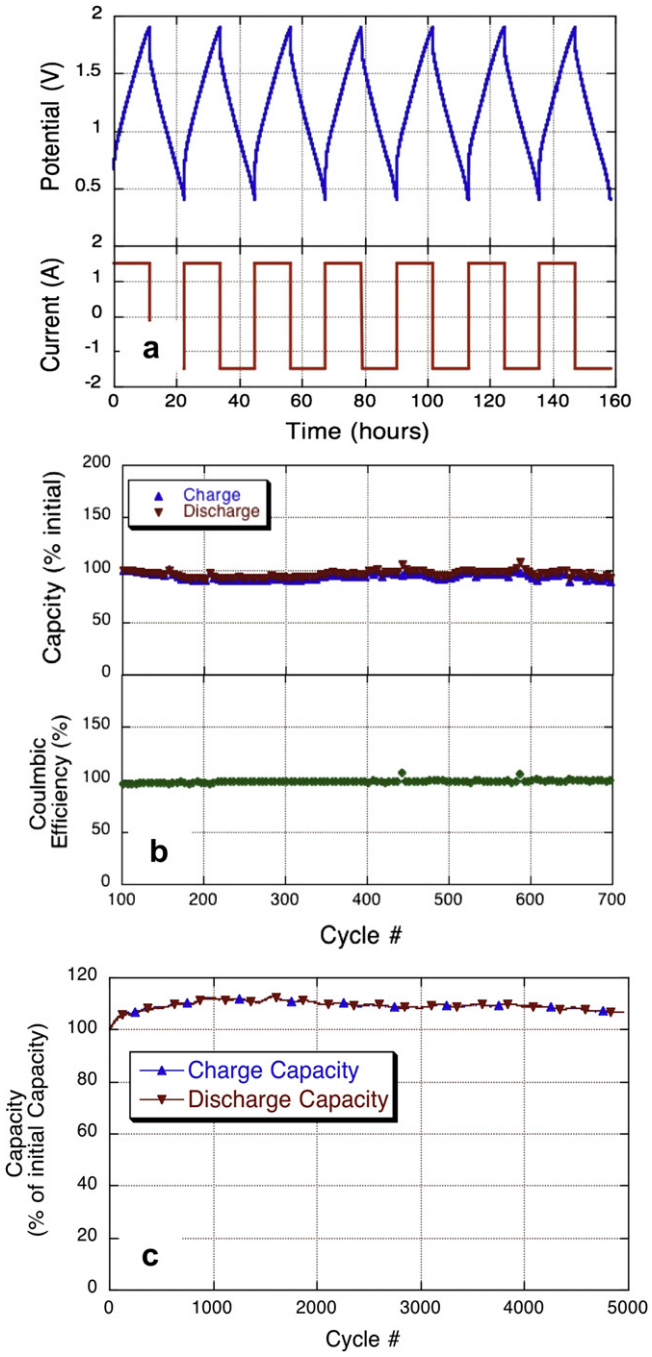

Fig. 7. Cycle life test data. (a) Typical lifecycle test profile for a large format, thick electrode test cell cycled at ~10 h rate. (b) Data from 700 cycles of a similar cell over 18 months of 100% DoD cycling. Little to no capacity fade is observed, and the columbic efficiency is >99%. (c) High rate cycle life testing on a thin electrode cells; 5000 cycles without loss in initial capacity.

repeated rapid cycling, a 2032 coin cell was made with electrodes <100 μm in thickness. Data from 10 min duration charge/discharge cycling (20 min per cycles) over is shown for 5000 cycles in Fig. 7(c). At these current rates, for electrodes with this form factor, it is estimated that approximately 70% of the active material is participating in the charge/discharge reaction. Again, no loss in capacity is observed, showing that active materials can be exercised extensively without significant materials degradation.

3.7. Self-discharge

To be viable, a bulk energy storage technology must demonstrate the ability to hold charge over extended periods with little or no self-discharge. To examine the self-discharge characteristics of this device, an elevated temperature stand at open circuit test was performed. Specifically, a 1.4 A h cell was deep cycled 200 times over 845 h of testing at a temperature of 60 °C. The cell was then left to stand at open circuit for 40 h, and then the cycling was resumed. The data plotted in Fig. 8 indicate that the cell potential rose to a steady-state open circuit value of 1 V, and held this potential constant for 10's of hours. No loss in cell potential was observed, and there was no evidence of self-discharge, and the cell showed no loss of function as a result of this extended rest. Furthermore, cells with initial potentials of 1.4–1.5 V that have been placed on long-term observation have been found to have open circuit potentials of over 1.1 V after a year of storage at ambient temperatures, indicating an extremely slow rate of self-discharge.

3.8. Multi-cell prototype performance

The vast majority of applications require DC bus potentials of tens or hundreds of Volts, many electrochemical cells must be connected electronically in series. In this configuration, most battery chemistries require cell-to-cell (or grouped parallel) electronic battery management systems (BMS) that monitor each cell voltage and routinely correct cells that diverge in state of charge or ability to deliver necessary capacity. For scaled low cost stationary storage, the use of cell-level BMS would be cumbersome and too costly. We find, however, that the hybrid/asymmetric configuration used in this battery does not require a BMS to be stable over extended periods of use. As a case in point, the charge/discharge curve in Fig. 9(a) is for a 350 mA h, 10-cell battery galvanostatically cycled between 8 and 18 V (0.8 and 1.8 V per cell, on average), while Fig. 9(b) shows the potentials of the individual cells plotted together. Each cell in this battery is stable and there is no divergence in cell or string performance over multiple cycles. Fig. 9(c) is a plot of the discharge capacity as a function of cycle of this 10-cell battery when charged to 18, 19, and 20 V. The battery was completely stable at when the battery was charged to both 18 and 19 V; in this case the cells were each charged to approximately 1.9 V.

3.9. Large format prototype performance

Practical and manufacturable large format cells of this chemistry must be designed. To this end, we have developed a proof-of-concept, pre-product prototype, the Aquion Energy "Battery 0" hybrid ion battery (HIB). This unit has approximately 1 L of open volume inside its casing and houses 10–14 layers of anode/cathode pairs. The internal configuration consists of individual electrode layers assembled in opposing sheets that are then connected internally in parallel in a true prismatic geometry. This device is not optimized to minimize mass or external envelope volume, but is instead designed to allow a range of manufacturing and performance parameters to be probed as the first product-class battery is designed. Fig. 10(a) is an image of the unit, and Fig. 10(b) is a potential vs. discharged energy for a low-current galvanostatic discharge. Fig. 10(c) is a plot indicating the W h l^{-1} delivered from the electrode pairs used to make the cell. Ongoing cycle life studies on these units indicate similar stability and performance as observed in smaller prototype units.

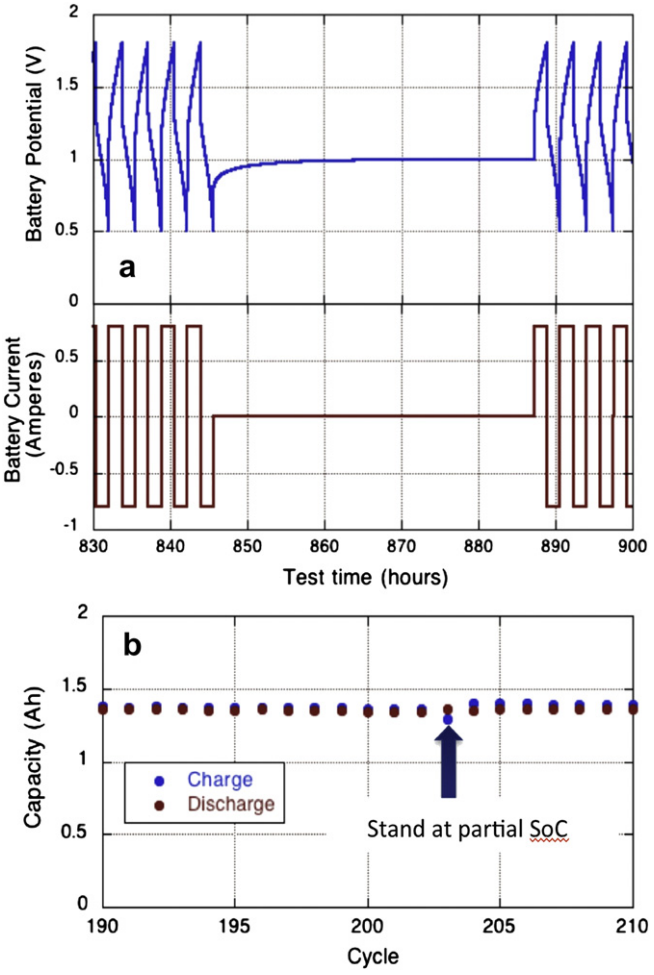

Fig. 8. Data indicating the performance of a typical device at 60 °C over 900 h. (a) The cell was cycled 202 times, and then left to stand at open circuit at a partial state of charge for 40 h, followed by resumed cycling. (b) Very little to no self-discharge was observed, and no loss in function occurred as a result of the stand at partial state of charge.

A 2.4 kW h, 80 V (max voltage) battery pack using two strings of 40 battery 0 units connected in parallel. There was no cell-level or string-level battery management electronics. After qualification, the pack was placed on a long-term application specific24-h duty profile provided by a company that designs and installs off-grid diesel/photovoltaic hybrid energy installations. Fig. 11 shows power demand as a function of time imparted on a lead acid battery pack used in the field. In this case, the magnitude of the load was scaled to the size of the pack such that a 75% state of charge swing would be encountered through each cycle. The maximum power was approximately 0.5 kW, and the total energy processed per day was 1.8 kW h. The voltage vs. time data shows that the system was extremely stable.

4. Discussion

A simple assessment focused on identifying the necessary performance parameters and costs of materials and subsequent

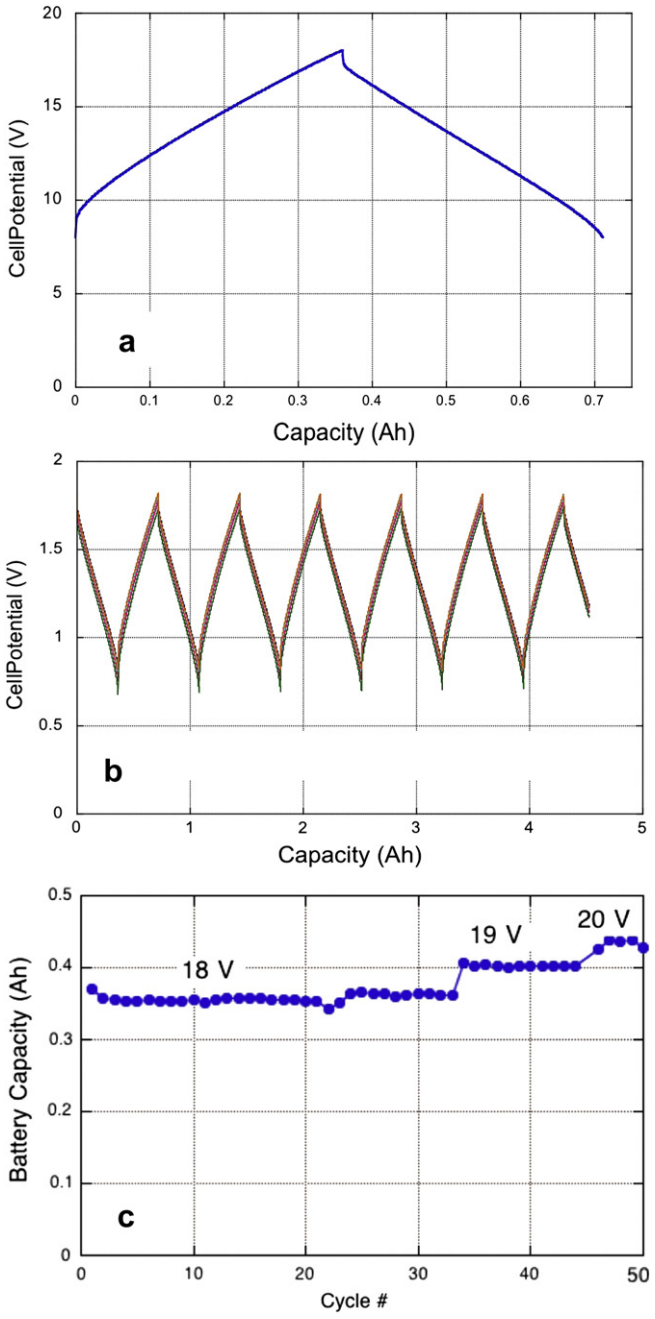

Fig. 9. Data showing performance of a string of ten 0.35 A h cells connected in series. (a) The charge discharge voltage profile under galvanostatic conditions (C/6 rate). (b) Plot showing the uniformity of the 10 cells during testing. (c) Capacity as function of cycle, with increasing maximum state of charge potential. The string was fully stable up to at least 2 V per cell.

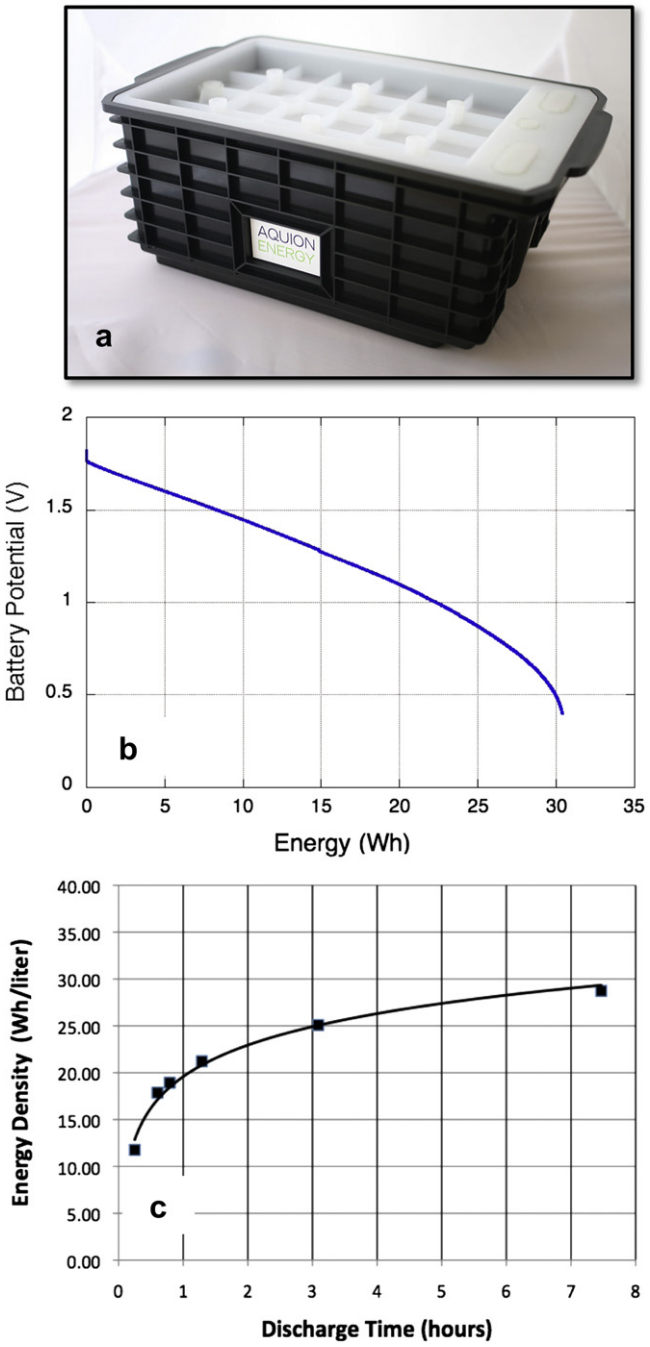

Fig. 10. (a) Image of engineering prototype "battery 0" unit. (b) 20 h galvanostatic discharge profile, plotted a potential vs. W h. delivered. (c) Relationship between discharge energy density of the battery 0 electrode stack as a function of discharge time.

devices for stationary energy storage applications has been described. By setting aside specific requirements for energy density and specific energy, and adopting cycle life, efficiency, and environmental constraints, we have arrived at a set of electrochemical couples that can be manufactured as freestanding thick format electrodes.

The data presented here indicate that the lithium-templated λ-MnO_2 can be cost effective as a positive electrode material when used in a neutral pH aqueous solution of Na_2SO_4. This is an expected result; previous results from electrochemical experiments on the cubic spinel λ-MnO_2in organic solvent based electrolyte using Na cations showed that there was a re-organization of the material into one of several lower capacity phases, including $Na_{0.7}MnO_2$ or the orthorhombic structured $Na_4Mn_9O_{18}$ [24]. The stability of this cathode material when used with Na cations in an aqueous solution is therefore unexpected, and must be related to the use of aqueous electrolyte. It is possible that proton or hydroxide species are introduced into the lattice, in part serving to stabilize the material against decomposition. It is also possible that the stability of the water/particle interface also contributes to this stability in the event that the nucleation of the degraded phase in the organic solvent electrolyte tests occurred on the external faces of the material when exposed to organic solvents.

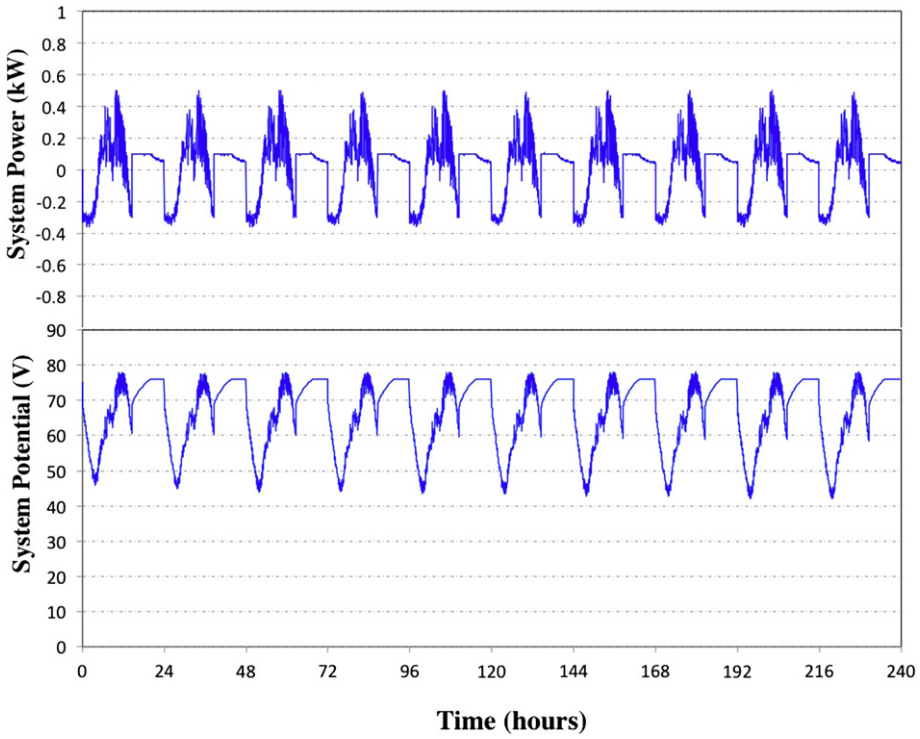

Fig. 11. System-level application-specific data showing the performance of a 60 V nominal, 2.4 kW h battery pack made of battery 0 units. This is a support profile for a diesel/PV/battery hybrid system. (a) The power vs. time profile recorded from a lead acid pack used in the field. (b) The resulting performance of the pack over 10 days of use.

A truly stable negative electrode material that has a reversible intercalation reactions with sodium (or other alkali elements) ions for >1000 cycles has yet to be identified, though there are some promising results based on various titanate system (it is not clear that the materials and processing costs of these materials would be sufficiently low). We show here, however, that activated carbon is completely stable and is able to function for the required number of cycles through the anodic potential range required by this device. Though many activated carbons that are tailored for organic solvent based electrochemical double layer capacitors can be very costly, up to \$100 kg^{-1} [25], we have found that suitable carbons for the sodium-ion chemistry can be made for much less from simple carbohydrate precursors. Ongoing work is focused on further augmenting the performance of low cost carbons and maximizing the effects of local hydrogen evolution and storage as a secondary storage mechanism.

The economics of this type of energy storage device are more appealing as electrode thicknesses are increased. However with thicker electrodes longer duration charge/discharge cycles are required to extract meaningful amounts of energy. The data in Figs. 5 and 6 show that, while there are limitations associated with ion transport in ultra thick electrode devices, it is possible to extract a large fraction of the total device energy in as little as 2 h. Many stationary storage applications require many hours of charging and discharging, and so it can be asserted here that there is a real market of devices such as the one described here that are tailored for duty cycles that require many hours for charging and discharging, and relatively low areal current densities for the current collector and tab structures within the battery. At higher charge/discharge rates, the device becomes less efficient largely through (electronic) resistive polarization, and as such there is the potential to use the device for higher rate applications that are not particularly sensitive to total round trip energy efficiency such as signal stabilization functions that require only multiple minutes of up/down regulation power.

The data presented here also show that high voltage strings are possible without relying on costly cell-level battery management equipment. This can be attributed to the unusually robust nature of the carbon negative electrode that is employed. Specifically – the data suggest that the negative electrode (anode) is stable to electrochemical bias potentials well below the expected values where electrolysis occurs. The combination of local surface/bulk storage of evolved hydrogen and the ability to consume that hydrogen upon discharge indicates that cells within a string that stray during use are able to self-regulate via this benign overcharge condition and as such should survive for extended periods of use. It has been found, in fact, that large format cell voltages in excess of 1.9 V can be obtained without significant decay in the performance of the device materials over many cycles.

Application specific testing on a large format pack made from manufacturing prototype units indicates that this approach can be practically scaled. Provided that the proper cost and price points can be achieved, there is a good chance that new class of energy storage devices will be implemented in a range of use cases.

5. Summary

Results from a project aimed at creating a highly stable large format energy storage device have been presented. A simple cost assessment shows that, for materials that may be practically expected to have extremely long cycle life, a materials cost of under \$5 to \$10 kg^{-1} at a device level is necessary, depending on the specific energy of the system. We propose that an aqueous electrolyte sodium-ion battery based on a positive electrode capable of sodium intercalation and capacitive/pseudocapacitive/hydrogen capturing negative electrode can reach this cost goal if the functional materials selected can be purchased and processed efficiently. Data presented here show that the cubic spinel λ-MnO_2 is sufficiently functional in a neutral pH Na_2SO_4 solution, and that some high surface area carbons that exhibit excellent performance

can be made from very inexpensive precursors. Thin electrode devices made from representative materials have excellent stability, cycle life, and round trip energy efficiencies (well above 90% even at rates in excess of 10C), while much more economically produced thick electrode devices retain appealing performance parameters if the charge and discharge durations experienced are greater than several hours. The performance of many of these devices connected in series is described and it is suggested that there is a cell-level overcharge reaction that can occur at the negative electrode that serves as an in-situ battery management system.

Acknowledgments

The authors wish to thank the following sources of funding rendered during the course of the work: Carnegie Mellon University, The Department of Energy (under the ARRA "Smart Grid Demonstration" program), Kleiner Perkins, Caufield and Byers, Foundation Capital, and ATV.

References

[1] L. Joerissen, J. Garche, C. Fabjan, G. Tomazic, Journal of Power Sources 127 (2004) 98–104.
[2] P.J. Hall, E.J. Bain, Energy Policy 36 (2008) 4352–4355.
[3] B. Scrosati, J. Garche, Journal of Power Sources 195 (2010) 2419–2430.
[4] P.S. Walmet, Sandia Publication Document SAND2009–5537, Evaluation of Lead/Carbon Devices for Utility Applications, Sandia National Lab, Albuquerque, New Mexico, 2009.
[5] X.C. Lu, G.G. Xia, J.P. Lemmon, Z.G. Yang, Journal of Power Sources 195 (2010) 2431–2442.
[6] M. Toupin, T. Brousse, D. Belanger, Chemistry of Materials 16 (2004) 3184–3190.
[7] Y.G. Wang, Y.Y. Xia, Journal of Electrochemical Society 153 (2006) A450–A454.
[8] C.D. Wessells, R.A. Huggins, Y. Cui, Nature Communications 2 (2011).
[9] J.Y. Luo, Y.Y. Xia, Advanced Functional Materials 17 (18) (2007) 3877–3884.
[10] S. Komaba, A. Ogata, T. Tsuchikawa, Electrochemical Communications 10 (2008) 1435–1437.
[11] J.C. Hunter, Journal of Solid State Chemistry 39 (1981) 142–147.
[12] S.B. Ma, K.W. Nam, W.S. Yoon, X.Q. Yang, K.Y. Ahn, K.H. Oh, K.B. Kim, Electrochemical Communications 9 (2007) 2807–2811.
[13] W.F. Wei, X.W. Cui, W.X. Chen, D.G. Ivey, Chemical Society Reviews 40 (2011) 1697–1721.
[14] A.D. Tevar, J.F. Whitacre, Journal of Electrochemical Society 157 (2010) A870–A875.
[15] J.F. Whitacre, A. Tevar, S. Sharma, Electrochemical Communications 12 (2010) 463–466.
[16] H. Manjunatha, G.S. Suresh, T.V. Venkatesha, Journal of Solid State Electrochemistry 15 (2011) 431–445.
[17] F. Beguin, K. Kierzek, M. Friebe, A. Jankowska, J. Machnikowski, K. Jurewicz, E. Frackowiak, Electrochimica Acta 51 (2006) 2161–2167.
[18] K. Jurewicz, E. Frackowiak, F. Beguin, Applied Physics A: Materials 78 (2004) 981–987.
[19] K. Jurewicz, E. Frackowiak, F. Beguin, Fuel Processing Technology 77 (2002) 415–421.
[20] D.Y. Qu, Journal of Power Sources 179 (2008) 310–316.
[21] S.E. Chun, Y.N. Picard, J.F. Whitacre, Journal of Electrochemical Society 158 (2011) A83–A92.
[22] J.W. Long, D. Belanger, T. Brousse, W. Sugimoto, M.B. Sassin, O. Crosnier, MRS Bulletin 36 (2011) 513–522.
[23] B. Dunn, H. Kamath, J.M. Tarascon, Science 334 (2011) 928–935.
[24] J.M. Tarascon, D.G. Guyomard, B. Wilkens, W.R. Mckinnon, P. Barboux, Solid State Ionics 57 (1992) 113–120.
[25] A. Burke, in: Proceedings of Vehicle Power and Propulsion, IEEE Conference, 2005, pp. 11–17.